Simplified mode analysis of guided mode resonance gratings with asymmetric coatings

Jun Wu (吴 俊), Changhe Zhou (周常河)*, Hongchao Cao (曹红超), Anduo Hu (胡安铎), Wenting Sun (孙文婷), and Wei Jia (贾 伟)

Laboratory of Information Optics and Opto-electronic Technology, Shanghai Institute of Optics and Fine Mechanics, Chinese Academy of Sciences, Shanghai 201800, China

**Corresponding author: chazhou@mail.shcnc.ac.cn*

Received January 21, 2013; accepted February 27, 2013; posted online April 29, 2013

A simplified modal method to explain the resonance phenomenon in guided mode resonance (GMR) gratings with asymmetric coatings is presented. The resonance observed is due to the interaction of two propagation modes inside the grating. The reflectivity spectra and electric field distributions calculated from the simplified modal method are compared using rigorous coupled-wave analysis (RCWA). The influences of high-order evanescent modes on the resonance peak are analyzed. A matrix Fabry-Perot (FP) resonance condition is developed to evaluate the resonance wavelength. An explanation for the resonance phenomenon observed based on the FP resonance phase condition is also proposed and demonstrated. The simplified method provides clear physical insights into GMR gratings that are useful for the analysis of a variety of other resonance gratings.

OCIS codes: 050.0050, 050.1950, 260.5740.
doi: 10.3788/COL201311.060501.

The modal method, first proposed by Botten *et al.* offers a simple and physical understanding of the diffraction process that takes place inside gratings[1]. However, while this method has long been proposed, it is not widely used. In 2005, Tishchenko restudied the modal method in deep lamellar gratings and proposed interesting concepts, such as impedance matching and a simplified modal method[2]. Clausnitzer *et al.* formally proposed a simplified modal method for a low-contrast transmission grating and designed highly efficient polarizing beam splitters[3,4]. Zheng *et al.* applied the modal method to design rectangular transmission gratings under second Bragg angle incidence and then designed a polarizing beam splitter with triangular-groove gratings[5,6].

The simplified modal method has been successfully applied in subwavelength low-contrast gratings. However, when the index contrast increases, such as when the refractive index of the grating bars n_{r} is around 2.0, as in guided mode resonance (GMR) filters with asymmetric coatings, obtaining diffraction efficiencies with simple equations is difficult. The same is true when the n_{r} of the grating bar ranges from 2.8 to 3.5, as in high broadband reflectors and high-quality factor resonators where the GMR gratings are considered high-contrast gratings (HCGs) but with symmetrical coatings. Moreover, consideration of the multiple reflections of grating modes inside the gratings and the corresponding coupling between modes for every reflection is necessary. Lalanne *et al.* proposed a coupled-Bloch-mode model to explain various optical properties of HCGs resulting from vertical resonances of coupled-resonator modes[7]. Karagodsky *et al.* proposed a simple analytical method to explain the ultra-high reflectivity feature of HCGs[8]. Based on the method proposed in Ref. [8], Karagodsky *et al.* presented a simple explanation for the multimode Fabry-Perot (FP) mechanism of resonant HCGs[9] and completely explained the extraordinary features of HCGs using a simple phase selection rule[10]. While the methods proposed in Refs. [7,8] mainly apply to HCGs with symmetric coatings, they are essentially variations of the simplified modal method.

The modal method proposed in Refs. [7–10] is applied to HCGs with symmetric coatings (also known as free-standing gratings) and has been successfully employed in vertical-cavity surface-emitting lasers and hollow-core low-loss waveguides[11−14]. However, for practical application, the gratings often have a substrate, i.e., GMR gratings with asymmetric coatings. Therefore, development of a simplified modal analysis for gratings with general structures, i.e., with asymmetric coatings, is necessary.

Asymmetrically coated GMR gratings, which consist of a diffraction grating and waveguide layers with a sharp peak in their reflective spectrum, have been extensively studied. They are used in laser cavity reflectors[15], light modulators[16], optical switch devices[17], polarizers[18], and narrowband filters[19]. The analytical method mainly employed for GMR gratings with asymmetric coatings at present is slab waveguide theory[20]. To date, no studies have investigated the resonance phenomenon in GMR gratings with asymmetric coatings using the simplified modal method.

In this letter, we develop the modal method proposed by Karagodsky[8−10] for HCGs with symmetric coatings. The method is applied to explain the resonance phenomenon in GMR gratings with asymmetrical coatings. In traditional discussions, where GMR occurs when the incident wave is coupled to a leaky lateral waveguide mode by phase-matching, attention is directed toward the lateral modes. By contrast, our discussion considers the phenomenon from an entirely different perspective and focuses on the interaction of longitudinal grating eigen modes. The proposed modal method with different numbers of modes is compared with the results of

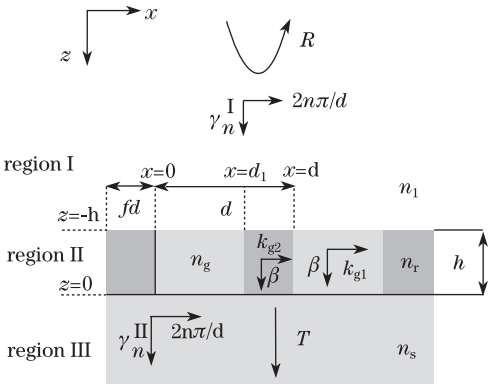

Fig. 1. Schematic of the guided mode resonance grating with nomenclature.

rigorous coupled-wave analysis (RCWA) simulation[21,22]. The influences of high-order evanescent modes on the resonance peak are also analyzed. The results of the simplified modal method and RCWA simulation agree well and validate the proposed method. Based on this method, a matrix FP resonance condition is developed for the GMR structure to evaluate the resonance wavelength. Finally, FP resonance phase conditions are proposed and demonstrated.

In this letter, we consider the case of normal incidence and transverse electric (TE) polarization (the electric field is in the y direction). Figure 1 shows the structure of a GMR grating with asymmetric coatings. n_1 and $n_{\mathtt{s}}$ are the refractive indices of the cover and substrate, respectively, $n_{\mathtt{r}}$ and $n_{\mathtt{g}}$ are the refractive indices of the grating bar and groove, respectively, d is the grating period, and h is the grating depth. The grating layer acts not only as a diffraction element but also as a waveguide layer. For GMR gratings with complex structures, where one or more waveguide layers are inserted between the grating and the substrate, the diffraction element and waveguide layers are separated.

The eigen equation for TE polarization is[2]

$$\cos k_{\mathtt{g}1}d_1 \cos k_{\mathtt{g}2}d_2 - \frac{1}{2}\left(\frac{k_{\mathtt{g}1}}{k_{\mathtt{g}2}} + \frac{k_{\mathtt{g}2}}{k_{\mathtt{g}1}}\right) \cdot \sin k_{\mathtt{g}1}d_1 \sin k_{\mathtt{g}2}d_2 = \cos k_x d, \tag{1}$$

where $d_1 = (1-f)d$, $d_2 = fd$, $k_x = k_0 n_1 \sin\theta$, θ is the angle of incidence, $k_{\mathtt{g}1} = \sqrt{(k_0 n_{\mathtt{g}})^2 - \beta^2} = k_0\sqrt{n_{\mathtt{g}}^2 - n_{\mathtt{eff}}^2}$, $k_{\mathtt{g}2} = \sqrt{(k_0 n_{\mathtt{r}})^2 - \beta^2} = k_0\sqrt{n_{\mathtt{r}}^2 - n_{\mathtt{eff}}^2}$, $n_{\mathtt{eff}}$ is the effective index of a mode, and $\beta = k_0 n_{\mathtt{eff}}$ is the propagation constant of a mode.

Under normal incidence, the equation can be split into two equations: one for even modes and the other for odd modes, which are described as

For even modes:

$$k_{\mathtt{g}1}\tan\frac{k_{\mathtt{g}1}d_1}{2} + k_{\mathtt{g}2}\tan\frac{k_{\mathtt{g}2}d_2}{2} = 0. \tag{2}$$

For odd modes:

$$k_{\mathtt{g}2}\tan\frac{k_{\mathtt{g}1}d_1}{2} + k_{\mathtt{g}1}\tan\frac{k_{\mathtt{g}2}d_2}{2} = 0. \tag{3}$$

Under normal incidence, Eq. (2) for even modes is identical to the dispersion relation of Ref. [8], which is obtained from the theory of periodic slab waveguide arrays. This relation illustrates that the analytical method presented in Ref. [8] is essentially the simplified modal method.

Under normal incidence, only the even modes can be excited because of symmetry. Given that odd modes cannot be excited, we only obtain even modes using Eq. (2). For a subwavelength dielectric grating, only a few propagating grating modes will dominate the diffraction process. Evanescent modes have little impact on the diffraction process. For the GMR grating studied in this letter, only two propagating modes occur in the wavelength range.

In the following discussion, we develop the analysis method proposed by Karagodsky *et al.*[8–10]. This modal method is mainly applicable to subwavelength HCGs with symmetric coatings, and the material of the grating groove is air[8–10]. A general simplified modal method for gratings with asymmetric coatings is presented. The grating modes are obtained by solving Eq. (2), after which electromagnetic boundary conditions at the grating-coating interfaces are matched to obtain the reflection and transmission efficiencies.

The basic formulas to be used are identical to those in Ref. [8], except for four differences. The first difference involves the lateral (x) wavenumbers ($k_{\mathtt{g}1}$ and $k_{\mathtt{g}2}$) inside the grating grooves and bars, which have been previously mentioned. The second difference involves the longitudinal (z) wavenumbers in regions I and III. For a grating with symmetric coatings, the longitudinal (z) wavenumbers in regions I and III are the same. However, for a grating with asymmetric coatings, the longitudinal (z) wavenumbers γ_n in regions I and III become

$$\gamma_n^{\mathrm{I}} = \sqrt{k_0^2 n_1^2 - (2n\pi/d)^2} = \sqrt{(2\pi/\lambda)^2 n_1^2 - (2n\pi/d)^2}, \tag{4}$$

$$\gamma_n^{\mathrm{III}} = \sqrt{k_0^2 n_2^2 - (2n\pi/d)^2} = \sqrt{(2\pi/\lambda)^2 n_2^2 - (2n\pi/d)^2}. \tag{5}$$

The third difference refers to the lateral (x) field profiles $h_{x,n}^{\mathrm{out}}$ and $e_{y,n}^{\mathrm{out}}$ in regions I and III. These profiles for symmetric coatings in Ref. [8] are identical. For asymmetric ones, however, these profiles are different.

In region I, they become

$$h_{x,n}^{\mathrm{I}} = \cos\left[(2n\pi/d)\,(x - d_1/2)\right], \quad e_{y,n}^{\mathrm{I}} = \left(-k_0/\gamma_n^{\mathrm{I}}\right)\eta h_{x,n}^{\mathrm{I}}. \tag{6}$$

In region III, they become

$$h_{x,n}^{\mathrm{III}} = \cos\left[(2n\pi/d)\,(x - d_1/2)\right], \quad e_{y,n}^{\mathrm{III}} = \left(-k_0/\gamma_n^{\mathrm{II}}\right)\eta h_{x,n}^{\mathrm{III}}. \tag{7}$$

Finally, the reflection matrices ρ at the boundaries of asymmetric coatings differ from those of symmetric ones. The ρ values for the top ($z = -h$) and bottom surfaces ($z = 0$) of a grating with symmetric coatings are identical in Ref. [8]. However, for a grating with asymmetric coatings, the ρ at $z = 0$ becomes

$$\rho_1 = \left(I + H_{\mathrm{III}}^{-1}E_{\mathrm{III}}\right)^{-1}\left(I - H_{\mathrm{III}}^{-1}E_{\mathrm{III}}\right). \tag{8}$$

The ρ at z = -h becomes

$$\rho_2 = \left(I + H_{\mathrm{I}}^{-1} E_{\mathrm{I}}\right)^{-1} \left(I - H_{\mathrm{I}}^{-1} E_{\mathrm{I}}\right). \tag{9}$$

Detailed derivations and definitions of η, ρ, H_{I}, E_{I}, H_{III}, and E_{III} may be found in Ref. [8].

To demonstrate the validity of the simplified modal method proposed above and determine how many modes are required to obtain good agreement with the RCWA simulation, we design a GMR grating and compare the reflective spectra calculated using the modal method and RCWA. The structural parameters of the designed grating are d = 363 nm, f = 0.5, h = 154.3 nm, n_1 = 1, n_{s} = 1.46, n_{r} = 2.1, and n_{g} = 2.0. The substrate material is quartz, i.e., SiO_2. The materials of the grating bar and groove may be zirconium dioxide and hafnium dioxide, respectively.

Figure 2(a) shows the reflectivities calculated using RCWA and the simplified modal method with the first two modes. The results of the two methods agree very well. Therefore, consideration of only the first two propagation modes in the simplified modal method presents sufficient precision to obtain the reflective spectrum.

To clearly present the difference between the two methods and analyze the influences of high-order evanescent modes to the resonance peak, we show the reflective spectra calculated using the two methods in Fig. 2(b) within a very narrow band. The results show that the shapes of the spectra are about the same but slightly shifted. The resonance wavelengths calculated by RCWA and the modal method with the first two, three, and four modes are 632.81, 633.16, 633.16, and 632.74 nm, respectively. The difference in wavelengths between RCWA and the modal method with the first two and three modes is 0.35 nm, which is larger than the difference in wavelengths obtained between RCWA and the modal method with four modes (0.07 nm). As the number of modes increases, the precision also increases. The first two modes are propagation modes, and the modes with orders larger than these are evanescent modes. For the resonance curve with a sharp peak, evanescent modes have certain effects on the position of the resonance peak, as shown in Fig. 2(b). The resonance wavelengths calculated using the modal method with the first two and three modes are about the same, so the third mode has little impact on the resonance peak. However, when the fourth mode is added to the calculations, the resonance peak shows a significant shift in contrast to the third mode. Thus, the fourth mode has more functions than the third one.

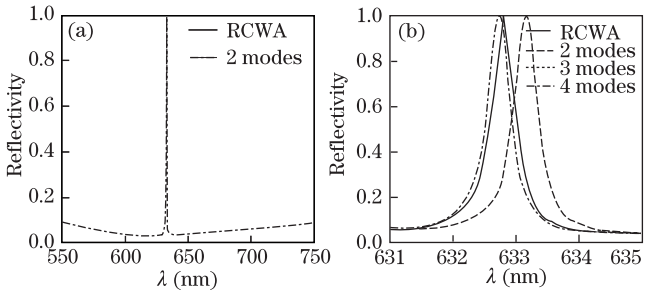

Fig. 2. (Color online) Reflective spectra calculated using RCWA and the modal method with (a) two modes and (b) different numbers of modes in a very narrow band.

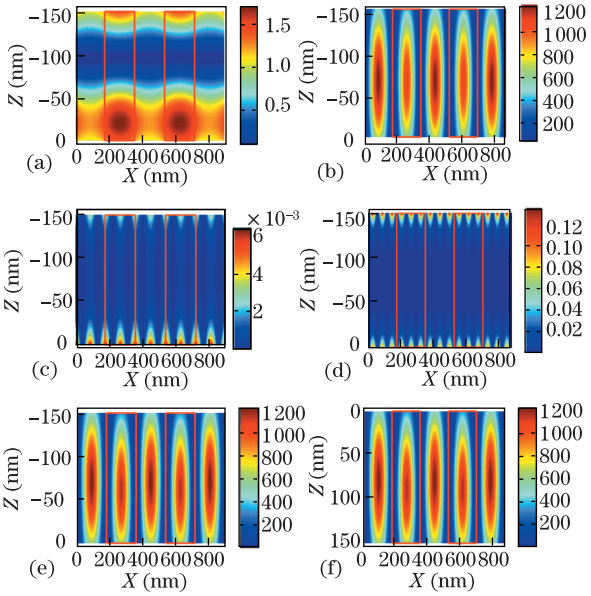

Fig. 3. (Color online) Electric field distributions of four grating modes: (a) the first $|E_1/E_0|^2$, (b) the second $|E_2/E_0|^2$, (c) the third $|E_3/E_0|^2$, and the (d) fourth $|E_4/E_0|^2$. Comparison of (e) the overall supermode $|E_{\mathrm{S}}/E_0|^2$ and (f) RCWA $|E_{\mathrm{R}}/E_0|^2$. Note: for RCWA, the origin of the z-axis is at the top surface of the grating.

Figures 3(a)–(d) show the electric field intensity distributions of the first four modes at a resonance wavelength of 632.74 nm. Figure 3(e) shows the overall electric field intensity of all four modes, which is defined as a supermode in Ref. [9]. Figure 3(f) shows the field intensity distribution calculated using RCWA with a resonance wavelength of 632.81 nm. All of these are normalized by the electric field intensity of the incident plane wave. The regions enclosed by the red boxes are grating bars. Figures 3(a)–(d) show that the first two grating modes are propagation waves and have a standing wave profile in the z direction. By contrast, the third and the fourth modes are surface evanescent waves, so their energies are confined close to the top and bottom of the grating. The intensities of the first two modes are much larger than those of the third and the fourth modes. This phenomenon indicates that the first two modes have major functions, especially the second mode, which has the largest electric field intensity. The intensities of the fourth mode are larger than those of the third mode. Thus, the fourth mode has a larger effect on the overall intensity than the third one. This result confirms the previous observation that the fourth mode has more effects on the resonance peak than the third one.

Figures 3(e) and (f) show that the intensity calculated using the modal method with the first four modes is identical to that obtained using the RCWA simulation with more Fourier modes at the resonance wavelength. The simplified modal method demonstrates favorable agreement with the RCWA simulation. In fact, the modal method with the first two modes yields intensities similar to those obtained using RCWA. Thus, simulations based on the modal method with only the first two modes show sufficient precision to analyze the resonance phenomenon. The resonance shown in Figs. 3(e) and (f) is

of the first-order type because only one peak along the z axis is observed for intensity.

For low-contrast transmission gratings, the grating modes excited at the cover-grating interface propagate forward and couple directly out to transmitted diffraction orders at the grating-substrate interface. The reflection and coupling between modes at the grating-substrate interface are very small; therefore, consideration of multiple reflections inside the grating region is not necessary. However, for HCGs, the reflection and coupling between modes at the boundaries are large because of the large index contrast, so the grating modes will be reflected multiple times inside the grating, just as in the case of FP effects.

Matrix FP resonance conditions can be developed from HCGs with symmetric coatings in Ref. [9] to the GMR gratings with asymmetric coatings discussed in this letter. The resonance phenomenon can be analyzed as follows. When the grating is illuminated by a plane wave, it can excite a collection of grating modes inside the grating with coefficients described by a vector $\mathbf{M} = (M_1, M_2, \ldots)^{\mathrm{T}}$, where M_n is the coefficient of the nth mode at the top surface of the grating ($z = -h$). Then, it propagates downward to the bottom surface of the grating ($z = 0$), where the weight vector becomes $\psi\mathbf{M}$. The modes are then reflected from the plane ($z = 0$) back up into the $-z$ direction with reflection matrix ρ_1 because of the large refractive index contrast between the grating and substrate. The weight vector now becomes $\rho_1\psi\mathbf{M}$. The modes propagate upward to the top surface of the grating and then are reflected from the plane ($z = -h$) back up into the $+z$ direction with reflection ρ_2 because of the large refractive index contrast between the grating and the cover. After one full round trip, the weight vector eventually becomes $\rho_2\psi\rho_1\psi\mathbf{M}$.

As stated in Ref. [9], resonance occurs when a collection of modes, $\mathbf{M}$, is self-sustainable. This condition can be clearly described by the expression: $\mathbf{M} = \rho_2\psi\rho_1\psi\mathbf{M}$. This expression means that after one full round trip, the supermode constructively interferes with itself, i.e., $(I - \rho_2\psi\rho_1\psi)\ \mathbf{M} = 0$, where I is a unit matrix. For a nonzero solution to exist in such a matrix equation, the determinant of the coefficient matrix should equal zero, i.e.,

$$\det\left(I - \rho_2\phi\rho_1\phi\right) = 0. \tag{10}$$

This is the resonance condition of GMR gratings with asymmetric coatings. Figure 4 shows $|\det(I - \rho_2\psi\rho_1\psi)|$ as a function of wavelength, which can be used for validating the resonance condition of GMR grating. The structural parameters of the grating are shown above, and the simulation is based on the double-mode modal method. As can be seen in Fig. 4, $|\det(I-\rho_2\psi\rho_1\psi)|$ shows a minimum at the wavelength of 633.16 nm, which is in accordance with the resonance wavelength obtained above. Therefore, Eq. (10) can be used to evaluate the resonance wavelength of GMR gratings with asymmetric coatings.

The proposed matrix resonance condition of GMR gratings considers the grating modes as a whole; the individual modes are not clear. Next, we discuss the phases of each mode. To simplify our analysis, we only consider the first two modes. After one full round trip, the weight vector is $\rho_2\psi\rho_1\psi\mathbf{M}$ and the accumulated phases are

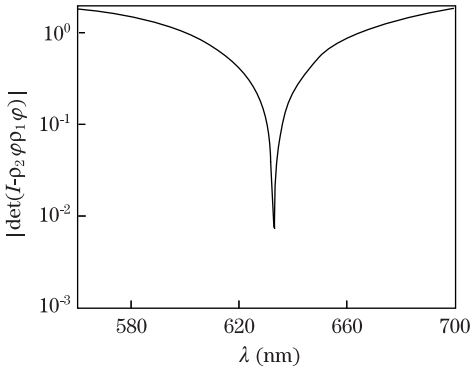

Fig. 4. $|\det(I - \rho_2\phi\rho_1\phi)|$ as a function of wavelength.

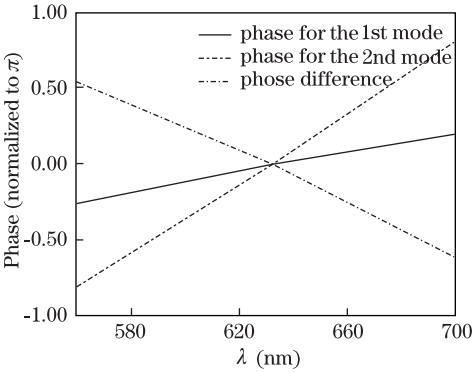

Fig. 5. (Color online) Phases of the first two modes and differences between them.

$$\psi_n = \text{phase (eigenvalue\# } n \quad of \quad \rho_2\psi\rho_1\psi\ ). \tag{11}$$

The FP phase resonance conditions for GMR gratings are

$$\begin{cases} \psi_n = 2m\pi \\ |\Delta\psi| = |\psi_2 - \psi_1| = 2l\pi \end{cases} \quad m, l = 0, 1, 2\cdots, \tag{12}$$

where n indicates the nth mode. Figure 5 shows the phases of the two modes during one round trip through the grating as well as their phase difference. The phase curves of the first two modes cross at a wavelength of about 633.16 nm. At this intersection, the phases of both modes equal $2m\pi$ ($m = 0, 1, 2, \cdots$). The phase difference between the two modes is also $2l\pi$ ($l = 0, 1, 2, \cdots$) at this point. At the resonance wavelength, the FP phase resonance conditions of Eq. (12) are fulfilled. When the phases of the two longitudinal propagation grating modes inside the grating simultaneously satisfy FP conditions, they interfere constructively. This phenomenon results in resonance inside the GMR grating, which clearly produces a physical picture of two-mode interference inside the grating.

In conclusion, we present a simplified modal method to explain the resonance phenomenon of GMR gratings with asymmetric coatings. The method focuses on the interaction of longitudinal grating modes inside the grating. The results of the simplified modal method and RCWA simulation agree very well with each other, which confirms the validity of the proposed method. Based on the double-mode modal method, a matrix FP resonance

condition is developed to evaluate the resonance wavelength. A FP resonance phase condition is proposed and demonstrated. This theoretical study provides a simple physical picture of resonance in GMR gratings that will be helpful for explaining resonance phenomena in other gratings with more complex structures.

This work was supported by the National Natural Science Foundation of China (Nos. 61078050, 60921004, and 61127013) and the Shanghai Science and Technology Committee (No. 11DZ2290302).

References

1. I. C. Botten, M. S. Craig, R. C. McPhedran, J. L. Adams, and J. R. Andrewartha, Opt. Acta **28,** 413 (1981).
2. A. V. Tishchenko, Opt. Quantum Electron. **37,** 309 (2005).
3. T. Clausnitzer, T. Kämpfe, E.-B. Kley, A. Tünnermann, U. Peschel, A. V. Tishchenko, and O. Parriaux, Opt. Express **13,** 10448 (2005).
4. T. Clausnitzer, T. Kämpfe, E.-B. Kley, A. Tünnermann, A. Tishchenko, and O. Parriaux, Appl. Opt. **46,** 819 (2007).
5. J. Zheng, C. Zhou, B. Wang, and J. Feng, J. Opt. Soc. Am. A **25,** 1075 (2008).
6. J. Zheng, C. Zhou, J. Feng, and B. Wang, Opt. Lett. **33,** 1554 (2008).
7. P. Lalanne, J. P. Hugonin, and P. Chavel, J. Lightwave Technol. **24,** 2442 (2006).
8. V. Karagodsky, F. G. Sedgwick, and C. J. Chang-Hasnain, Opt. Express **18,** 16973 (2010).
9. V. Karagodsky, C. Chase, and C. J. Chang-Hasnain, Opt. Lett. **36,** 1704 (2011).
10. V. Karagodsky and C. J. Chang-Hasnain, Opt. Express **20,** 10888 (2012).
11. M. C. Y. Huang, Y. Zhou, and C. J. Chang-Hasnain, Nat. Photon. **1,** 119 (2007).
12. M. C. Y. Huang, Y. Zhou, and C. J. Chang-Hasnain, Nat. Photon. **2,** 180 (2008).
13. Y. Zhou, V. Karagodsky, B. Pesala, F. G. Sedgwick, and C. J. Chang-Hasnain, Opt. Express **17,** 1508 (2009).
14. D. Fattal, J. Li, Z. Peng, M. Fiorentino, and R. G. Beausoleil, Nat. Photon. **4,** 466 (2010).
15. T. Kobayashi, Y. Kanamori, and K. Hane, Appl. Phys. Lett. **87,** 151106 (2005).
16. T. Katchalski, G. Levy-Yurista, A. Friesem, G. Martin, R. Hierle, and J. Zyss, Opt. Express **13,** 4645 (2005).
17. A. Mizutani, H. Kikuta, and K. Iwata, J. Opt. Soc. Am. A **22,** 355 (2005).
18. E. N. Glytsis and T. K. Gaylord, Appl. Opt. **31,** 4459 (1992).
19. S. Tibuleac and R. Magnusson, J. Opt. Soc. Am. A **14,** 1617 (1997).
20. S. S. Wang and R. Magnusson, Appl. Opt. **32,** 2606 (1993).
21. M. G. Moharam, E. B. Grann, D. A. Pommet, and T. K. Gaylord, J. Opt. Soc. Am. A **12,** 1068 (1995).
22. P. Lalanne and G. M. Morris, J. Opt. Soc. Am. A **13,** 779 (1996).